

Biomass burning sources control ambient particulate matter but traffic and industrial sources control VOCs and secondary pollutant formation during extreme pollution events in Delhi

Arpit Awasthi¹, Baerbel Sinha¹, Haseeb Hakkim¹, Sachin Mishra¹, Varkrishna Mummidivarapu¹, Gurmanjot Singh¹, Sachin D. Ghude², Vijay Kumar Soni³, Narendra Nigam³, Vinayak Sinha¹, Madhavan N. Rajeevan⁴

¹Department of Earth and Environmental Sciences, Indian Institute of Science Education and Research Mohali, Sector 81, S.A.S Nagar, Manauli PO, Punjab, 140306, India

²Indian Institute of Tropical Meteorology, Pashan, Pune 411 008, Ministry of Earth Sciences, India

³India Meteorological Department, New Delhi 110 003, Ministry of Earth Sciences, India

⁴Ministry of Earth Sciences, Government of India, New Delhi 110 003, India

Correspondence to: Baerbel Sinha (bsinha@iisermohali.ac.in)

Table S1: 111 NMVOCs species used in the PMF model, the table lists the major compound identifications and the references supporting such assignments from previous works along with detection limits.

Sr. No	Protonated m/z	Potential contributor	Strong /Weak	Mean (with range) $\mu\text{g}/\text{m}^3$	Sources	References
1	31.014	Formaldehyde CH_2O	Strong	1.063 (0.066-9.464)	Photochemical production, traffic, biomass burning	Hatch et al. 2015, Stockwell et al. 2015, Koss et al. 2018
2	33.030	Methanol CH_4O	Strong	17.285 (3.522-127.853)	Photochemical production, biomass burning, biogenic	Hatch et al. 2015, Stockwell et al. 2015, Koss et al. 2018
3	41.035	Propyne C_3H_4	Strong	9.149 (1.001-96.661)	Traffic, biomass burning	Hatch et al. 2015, Stockwell et al. 2015, Koss et al. 2018, Hakkim et al. 2021
4	42.030	Acetonitrile $\text{C}_2\text{H}_3\text{N}$	Strong	0.888 (0.208-5.208)	Biomass burning, industries	Hatch et al. 2015, 2017
5	43.051	Propene C_3H_6	Strong	5.117 (0.766-59.931)	Biomass burning, traffic	Hakkim et al. 2021
6	44.018	Isocyanic acid HNCO	Strong	0.145 (0.007-1.231)	Oxidation of amines (secondary formation), biomass burning	Chandra & Sinha, 2016; Wang et al., 2020
7	45.030	Acetaldehyde $\text{C}_2\text{H}_4\text{O}$	Strong	8.764 (1.432-55.175)	Biogenic, biomass burning, photochemical	Hatch et al. 2015, Stockwell et al. 2015, Koss et al. 2018, Kumar et al.

					production	2021
8	46.025	Formamide CH ₄ NO	Strong	0.447 (0.004-8.3)	Oxidation of amines (secondary formation)	Yao et al. 2016; Wang et al. 2022
9	47.009	Formic acid CH ₂ O ₂	Strong	1.717 (0.004-31.063)	Oxidation of amines (secondary formation)	Yao et al. 2016; Wang et al. 2022
10	47.0457	Ethanol C ₂ H ₆ O	Strong	0.625 (0.052-7.845)	Industrial, Traffic	Bruns et al. 2017; Koss et al. 2018
11	48.048	methoxyamine CH ₅ NO	Weak	0.011 (0-0.148)	Oxidation of amines (secondary formation)	Yáñez-Serrano et al. 2021
12	49.007	Methanethiol CH ₄ S	Strong	0.15 (0.002-3.295)	Industrial	Toda et. al. 2010
13	53.035	Vinylacetylene, 1-Buten-3-yne C ₄ H ₄	Strong	0.662 (0.003-10.879)	Biomass burning	Hatch et al. 2015, Stockwell et al. 2015, Koss et al. 2018
14	55.051	1,2-Butadiene, 1-Butyne, 2-Butyne, 1,3 Butadiene C ₄ H ₆	Strong	3.701 (0.418-30.204)	Biomass burning	Koss et al., 2018, Sarkar et al., 2017
15	57.030	Acrolein C ₃ H ₄ O	Strong	0.802 (0-8.038)	Biomass burning, waste burning	Kumar et al. 2021
16	57.067	Methyl tert-butyl ether (MTBE) fragment /Butene C ₄ H ₈	Strong	7.293 (0.983-100.664)	Biomass burning, waste burning, traffic	Hakkim et al. 2021
17	59.046	Acetone + Propanal C ₃ H ₆ O	Strong	14.603 (2.341-145.458)	Biomass burning, industries, photochemical production	Hatch et al. 2015, Stockwell et al. 2015, Koss et al. 2018, Kumar et al. 2021
18	61.025	Acetic acid+ Glycolaldehyde C ₂ H ₄ O ₂	Strong	16.086 (0.695-170.723)	Photochemical production, biomass burning, industries	Kumar et al. 2021
19	62.997	Vinyl chloride C ₂ H ₃ Cl	Weak	0.02 (0.001-0.235)	PVC burning	Hsu et. al. 2022, Fukusaki et al. 2021
20	67.051	Cyclopentadiene, monoterpene fragment, butanol fragment C ₅ H ₆	Strong	0.781 (0.117-10.93)	Biomass burning	Hatch et al. 2015; Stockwell et al., 2015
21	69.031	Furan C ₄ H ₄ O	Strong	0.231 (0.011-3.247)	Biomass burning	Coggon et al., 2019; Hatch et al. 2015; 2017; Koss et al., 2018; Stockwell et al., 2015
22	69.067	Isoprene + 2-methyl-3-butene-2-ol fragment C ₅ H ₈	Strong	2.234 (0.294-17.733)	Biogenic sources, biomass burning	Stockwell et al., 2015; Jordan et al., 2009
23	71.047	Methyl Vinyl Ketone, Methacrolein, Butenal	Strong	1.015 (0.099-4.729)	Biomass burning,	Stockwell et al., 2015; de

		C ₄ H ₆ O			photochemical production	Gouw et al., 2007
24	73.026	Methyl glyoxal C ₃ H ₄ O ₂	Strong	0.56 (0.004-8.797)	Oxidation of amines (secondary formation)	Yao et al. 2016; Wang et al. 2022
25	73.062	Butanal, Butanone, MEK C ₄ H ₈ O	Strong	2.534 (0.315-43.128)	Biomass burning, biogenic, photochemical production	Hatch et al. 2015, Stockwell et al. 2015, Koss et al. 2018
26	75.042	Hydroxyacetone/ Propanoic acid C ₃ H ₆ O ₂	Strong	1.664 (0.116-14.045)	Biomass burning, biogenic, traffic	Kumar et al. 2021
27	76.037	Nitroethane C ₂ H ₅ NO ₂	Strong	0.036 (0.002-0.308)	Biomass burning	Palm et al. 2020, Harrison et al. 2005
28	79.052	Benzene C ₆ H ₆	Strong	6.07 (0.305-68.694)	Biomass burning, traffic	Hatch et al. 2015, Stockwell et al. 2015, Koss et al. 2018, Hakkim et al. 2021
29	81.031	Cyclopentadienone C ₅ H ₄ O	Strong	0.102 (0.001-0.896)	Biomass burning	Hatch et al. 2015, Koss et al. 2018; Nowakowska et al. 2018
30	83.047	Methyl furan C ₅ H ₆ O	Strong	0.363 (0.032-3.68)	Biomass burning	Coggon et al., 2019; Hatch et al. 2015; 2017; Koss et al., 2018; Stockwell et al., 2015
31	83.084	Cyclohexene, Hexyne isomers C ₆ H ₁₀	Strong	1.406 (0.345-12.044)	Biomass burning, biogenic, traffic	Stockwell et al., 2015, Koss et al., 2018; Kumar et al., 2021;
32	84.080	Pentanenitrile/ Methylbutanenitrile isomers/ C5-amines C ₅ H ₉ N	Strong	0.037 (0-0.495)	Biogenic, biomass burning	Hatch et al. 2015, 2017
33	85.027	Furanone / butenedial C ₄ H ₄ O ₂	Strong	0.466 (0.015-6.719)	Biomass burning, photochemical production	Coggon et al., 2019; Hatch et al. 2015; 2017; Koss et al., 2018; Stockwell et al., 2015
34	85.063	Cyclopentanone C ₅ H ₈ O	Strong	0.337 (0.042-1.971)	Biomass burning, traffic	Hatch et al. 2015, Koss et al. 2018; Nowakowska et al. 2018
35	85.094	Cyclohexane, Hexene C ₆ H ₁₂	Strong	0.326 (0.051-4.057)	Biomass burning, Traffic	Fleming et al. 2018, Hakkim et al. 2021
36	87.043	Isomers of C4 carboxylic acid/ester/diketone C ₄ H ₆ O ₂	Strong	1.118 (0.06-8.545)	Biomass burning, photochemical production	Kumar et al. 2021, Hatch et al. 2015, Koss et al. 2018; Nowakowska et al. 2018
37	87.079	Pentanone, methyl-buteneol, Pentanal C ₅ H ₁₀ O	Strong	0.295 (0.05-1.841)	Biomass burning, biogenic	Hatch et al. 2015, Stockwell et al. 2015, Koss et al. 2018

38	89.058	Isomers of C4-carboxylic acid/ester C ₄ H ₈ O ₂	Strong	1.306 (0.087-17.301)	Industrial solvent	Kamarulzaman et al. 2019
39	91.053	Monoterpene Fragment C ₇ H ₆	Strong	1.24 (0.058-20.618)	Industrial, Traffic	Kamarulzaman et al. 2019
40	93.069	Toluene C ₇ H ₈	Strong	18.285 (0.43-321.651)	Biomass burning traffic, chemical production, biogenic	Hatch et al. 2015, Stockwell et al. 2015, Koss et al. 2018, Hakkim et al. 2021
41	95.048	Phenol C ₆ H ₆ O	Strong	0.835 (0.069-9.968)	Biomass burning, photochemical production	Hakkim et al., 2021; Koss et al., 2018; Kumar et al., 2021
42	95.084	Monoterpene Fragment C ₇ H ₁₀	Strong	0.826 (0.111-13.348)	Industrial, traffic	Kamarulzaman et al. 2019
43	97.027	Furfural/ isomers of diketone/carboxylic acid/ester C ₅ H ₄ O ₂	Strong	0.649 (0.026-17.29)	Biomass burning	Kumar et al. 2021, Coggon et al., 2019; Hatch et al. 2015; 2017; Koss et al., 2018; Stockwell et al., 2015
44	97.063	C2 substituted furan, methyl Cyclopentenone C ₆ H ₈ O	Strong	0.277 (0.024-2.555)	Biomass burning	Coggon et al., 2019; Hatch et al. 2015; 2017; Koss et al., 2018; Stockwell et al., 2015
45	97.100	Cycloheptene, Alkyl fragment C ₇ H ₁₂	Strong	0.634 (0.104-7.483)	Biomass burning	Stockwell et al., 2015; Koss et al., 2018; Kumar et al., 2021
46	99.043	Furfuryl alcohol, Methyl-furanone C ₅ H ₆ O ₂	Strong	0.599 (0.025-4.61)	Photochemical production, Biomass burning	Coggon et al., 2019; Hatch et al. 2015; 2017; Koss et al., 2018; Stockwell et al., 2015
47	99.079	Cyclohexanone/isomers of C6-aldehyde/ketone C ₆ H ₁₀ O	Strong	1.033 (0.088-23.49)	Industrial	Gupta et al. 1979
48	99.116	Methylcyclohexane, Heptene & other hydrocarbons C ₇ H ₁₄	Weak	0.034 (0.002-0.472)	asphalt degassing	Khare et al., 2020
49	101.059	Pentanedione/ isomers of C5-diketone/carboxylic acid/ester/aldehyde C ₅ H ₈ O ₂	Strong	0.777 (0.048-5.073)	Biomass burning	Hatch et al. 2015, Koss et al. 2018; Nowakowska et al. 2018
50	105.069	Styrene C ₈ H ₈	Strong	1.556 (0.13-35.843)	Biomass burning traffic, chemical production	Jordan et al., 2009; Stockwell et al., 2015
51	107.050	Benzaldehyde/ isomers of C7-aldehyde/ ketone C ₇ H ₆ O	Strong	0.484 (0.003-4.687)	Biomass burning, photochemical production	Hatch et al. 2015, Stockwell et al. 2015, Koss et al. 2018

52	107.085	Sum of C8-Aromatics C ₈ H ₁₀	Strong	11.214 (0.4-193.065)	Biomass burning, traffic	Hatch et al. 2015, Stockwell et al. 2015, Koss et al. 2018, Hakkim et al. 2021
53	109.064	Methylphenol isomers, Anisole C ₇ H ₈ O	Strong	0.24 (0.021-2.61)	Biomass Burning	Hatch et al. 2015
54	109.100	Terpene fragment/Cyclooctadiene C ₈ H ₁₂	Strong	0.511 (0.089-5.681)	Industrial, traffic	Kamarulzaman et. al. 2019
55	111.042	Methylfurfural, Hydroxyphenol C ₆ H ₆ O ₂	Strong	0.208 (0.002-4.11)	Biomass burning, photochemical production	Coggon et al., 2019; Hatch et al. 2015; 2017; Koss et al., 2018; Stockwell et al., 2015
56	111.080	C3-substituted furans, C2- substituted cyclopentene, methyl cyclohexene C ₇ H ₁₀ O	Strong	0.195 (0.024-1.519)	Biomass burning	Coggon et al., 2019; Hatch et al. 2015; 2017; Koss et al., 2018; Stockwell et al., 2015
57	111.116	Ethenyl cyclohexane C ₈ H ₁₄	Strong	0.434 (0.078-5.193)	Ring-opening products of cyclic alkanes	Wang et. al. 2015
58	113.059	Dimethylbutenedial / C4- substituted aldehyde C ₆ H ₈ O ₂	Strong	0.403 (0.023-2.736)	Oxidation of aromatic compounds, biomass burning	Zaytsev et al., 2019
59	115.039	Hydroxymethyl furanone/ methylepoxybutanedial C ₅ H ₆ O ₃	Strong	0.119 (0.004-1.797)	Photochemical production, Biomass burning	Coggon et al., 2019; Hatch et al. 2015; 2017; Koss et al., 2018; Stockwell et al., 2015
60	115.075	Isomers of C6- diketones/aldehyde/carbo xylic acid/ester C ₆ H ₁₀ O ₂	Strong	0.357 (0.024-2.187)	Oxidation of polyaromatic hydrocarbons	Bruns et al. 2017
61	116.108	C6-amides C ₆ H ₁₃ NO	Weak	0.035 (0-0.255)	Photooxidation of amines	Yao et al. 2016
62	119.085	Terpene fragment C ₉ H ₁₀	Strong	0.608 (0.062-9.105)	Traffic	Erickson et. al. 2013
63	121.064	Tolualdehyde/ isomers of C8-aldehyde/ketone C ₈ H ₈ O	Strong	0.578 (0.048-6.186)	Biomass burning	Hatch et al. 2015, Koss et al. 2018
64	121.101	Sum of C-9 aromatics C ₉ H ₁₂	Strong	5.67 (0.174-125.472)	Traffic, Biomass burning	Hatch et al. 2015, Stockwell et al. 2015, Koss et al. 2018
65	123.044	Hydroxybenzaldehyde/iso mers of C7- carboxylic acid/ ester C ₇ H ₆ O ₂	Strong	0.307 (0.009-2.77)	Photochemical production, Biomass burning	Hatch et al. 2015, Koss et al. 2018; Nowakowska et al. 2018
66	123.080	C2-substituted phenol, methyl anisole C ₈ H ₁₀ O	Strong	0.146 (0.013-1.255)	Oxidation of polyaromatic hydrocarbons	Bruns et al. 2017
67	123.12	Santene, Cyclopentadiene	Strong	0.349	asphalt	Khare et al., 2020,

		& other hydrocarbons C ₉ H ₁₄		(0.063-3.73)	degassing	Kılıç et al., 2018
68	124.039	Nitrobenzene C ₆ H ₅ NO ₂	Strong	0.054 (0.004-0.871)	Traffic	Palm et al. 2020, Harrison et al. 2005
69	125.060	Guaiacol/ isomers of C7- carboxylic acid/ester C ₇ H ₈ O ₂	Strong	0.162 (0.01-2.15)	Biomass burning	Hatch et al. 2015, Koss et al. 2018; Nowakowska et al. 2018
70	125.133	Nonyne, nondiene C ₉ H ₁₆	Strong	0.157 (0.033-1.702)	asphalt degassing	Khare et al., 2020, Kılıç et al., 2018
71	127.039	Hydroxymethyl furfural C ₆ H ₆ O ₃	Strong	0.116 (0.004-2.045)	biomass burning	Koss et al., 2018
72	127.075	Isomers of C7-carboxylic acid/ester/ aldehyde/ketone C ₇ H ₁₀ O ₂	Strong	0.226 (0.014-1.5)	Oxidation of aromatic compounds, biomass burning	Zaytesv et al., 2019
73	129.070	Naphthalene C ₁₀ H ₈	Strong	1.043 (0.099-12.618)	Traffic, biomass burning	Hakkim et al., 2021; Koss et al., 2018; Kumar et al., 2021
74	129.092	Isomers of C9- acetaldehyde/ ketone/ Carboxylic acid/ester C ₇ H ₁₂ O ₂	Strong	0.176 (0.01-1.274)	Oxidation of polyaromatic hydrocarbons	Bruns et al. 2017, Lignell et al. 2013
75	133.065	Methyl benzofuran C ₉ H ₈ O	Strong	0.078 (0.007-0.617)	Biomass Burning	Hatch et al. 2015
76	133.102	Ethyl styrene, tetrahydronaphthalene C ₁₀ H ₁₂	Strong	0.457 (0.044-7.886)	Traffic	Yáñez-Serrano et al. 2021
77	135.080	Isomers of C9- acetaldehyde/ ketone C ₉ H ₁₀ O	Strong	0.172 (0.007-1.367)	Traffic	Knighton et. al. 2007
78	135.118	P-cymene, C4-substituted benzene, C2-substituted xylene C ₁₀ H ₁₄	Strong	2.509 (0.091-71.697)	Traffic	Hakkim et al. 2021
79	137.133	Sum of Monoterpenes (MT) C ₁₀ H ₁₆	Strong	2.66 (0.167-127.676)	Industrial, biogenic, biomass burning, traffic	Guenther et al., 2006; Kamarulzaman et. al. 2019 Koss et al., 2018; Kumar et al., 2021
80	138.056	Nitrotoluene/ salicylamide C ₇ H ₇ NO ₂	Weak	0.036 (0.001-0.707)	Oxidation of toluene	Ramasamy et al., 2019
81	143.086	Methyl naphthalene C ₁₁ H ₁₀	Strong	0.19 (0.015-2.848)	Biomass Burning, Traffic	Hatch et al. 2015; Yáñez-Serrano et al. 2021
82	143.108	Isomers of C8- aldehyde/ketone/carboxylic acid /ester C ₈ H ₁₄ O ₂	Strong	0.153 (0.022-0.942)	Oxidation of polyaromatic hydrocarbons	Bruns et al. 2017
83	145.051	Organic acids/ levoglucosan fragment C ₆ H ₈ O ₄	Strong	0.068 (0.002-1.626)	Biomass Burning	Hatch et al. 2015, Koss et al. 2018; Nowakowska et al. 2018

84	145.102	C2-substituted indene C ₁₁ H ₁₂	Weak	0.062 (0.007-0.814)	Asphalt degassing	Khare et al., 2020
85	145.123	Isomer of C8-carboxylic acid/ C8-ester C ₈ H ₁₆ O ₂	Strong	0.072 (0.003-0.96)	Oxidation of polyaromatic hydrocarbons	Bruns et al. 2017, Mochizuki et al. 2019
86	146.977	Isomers of Dichlorobenzene C ₆ H ₄ Cl ₂	Strong	0.352 (0.009-5.79)	Industrial pesticides	Graus et al. 2010, Yáñez-Serrano et al. 2021
87	147.118	Cyclopentylbenzene & other hydrocarbons C ₁₁ H ₁₄	Strong	0.318 (0.038-4.599)	asphalt degassing	Khare et al., 2020
88	149.024	Phthalic anhydride/Benzofurandione C ₈ H ₄ O ₃	Strong	0.195 (0.003-4.508)	Oxidation of polyaromatic hydrocarbons	Bruns et al. 2017
89	149.096	Isomers of C10-aldehyde/ ketone C ₁₀ H ₁₂ O	Strong	0.094 (0.008-1.25)	asphalt degassing	Khare et al., 2020
90	153.092	Isomers of C9- carboxylic acid/ester C ₉ H ₁₂ O ₂	Strong	0.102 (0.01-1.413)	Oxidation of monoterpenes	Gkatzelis et al. 2018
91	153.128	Isomers of C10-aldehyde/ ketone C ₁₀ H ₁₆ O	Strong	0.31 (0.021-7.93)	Oxidation of monoterpenes	Camredon et al.: 2010
92	154.052	Nitrobenzyl alcohol/Nitrocresols, methyl-nitrophenol C ₇ H ₇ NO ₃	Strong	0.077 (0.003-0.577)	Oxidation of toluene	Ramasamy et al., 2019
93	155.108	Isomers of C9-ketone/ C9-carboxylic acid/ C9-ester C ₉ H ₁₄ O ₂	Strong	0.104 (0.008-0.759)	Oxidation of monoterpenes	Camredon et al.: 2010, Gkatzelis et al. 2018
94	155.144	Isomers of C10-aldehyde/ketone C ₁₀ H ₁₈ O	Strong	0.092 (0.008-1.238)	asphalt degassing	Khare et al., 2020
95	157.099	C2-substituted naphthalene C ₁₂ H ₁₂	Strong	0.144 (0.017-1.209)	asphalt degassing	Khare et al., 2020, Kılıç et al., 2018
96	157.122	C9-ester/C9-organic acid C ₉ H ₁₆ O ₂	Strong	0.109 (0.012-1.035)	Oxidation of monoterpenes	Lignell et al. 2013; Camredon et al. 2010
97	159.140	C9-organic acid C ₉ H ₁₈ O ₂	Weak	0.056 (0.002-0.559)	Oxidation of monoterpenes	Mochizuki et al. 2019
98	161.134	Cyclohexylbenzene, butyl styrene, cyclopentylmethylbenzene C ₁₂ H ₁₆	Strong	0.161 (0.016-2.527)	asphalt degassing	Khare et al., 2020 Kılıç et al., 2018
99	175.150	Trimethyltetralin/ ionene C ₁₃ H ₁₈	Strong	0.086 (0.007-1.677)	asphalt degassing	Khare et al., 2020
100	177.056	Formylcinnamic acid / hydroxy-methyl-coumarin C ₁₀ H ₈ O ₃	Strong	0.105 (0.006-0.852)	asphalt degassing	Xing et al. 2023
101	177.165	C7-substituted benzene, C ₁₃ H ₂₀	Strong	0.13 (0.013-2.594)	asphalt degassing	Khare et al., 2020
102	179.181	C3-substituted adamantane C ₁₃ H ₂₂	Weak	0.06 (0.006-0.878)	asphalt degassing	Khare et al., 2020

103	183.121	Bibenzyl C ₁₄ H ₁₄	Weak	0.029 (0.004-0.2)	asphalt degassing	Khare et al., 2020
104	185.121	cis-Pinonic acid / C10-ester C ₁₀ H ₁₆ O ₃	Weak	0.054 (0.007-1.571)	Oxidation of monoterpenes	Camredon et al. 2010, Khare et. al. 2020
105	187.148	C4-substituted dihydroazulene, benzyl cycloheptene C ₁₄ H ₁₈	Weak	0.039 (0.005-0.306)	asphalt degassing	Khare et al. 2020, Loubet et al. 2022
106	189.165	C4-substituted dihydronaphthalene, cyclopentylpropylbenzene C ₁₄ H ₂₀	Weak	0.053 (0.006-0.818)	asphalt degassing	Khare et al., 2020
107	191.181	C8-substituted benzene C ₁₄ H ₂₂	Weak	0.068 (0.007-0.892)	asphalt degassing	Khare et al., 2020
108	195.138	Myrtenyl acetate/C12- organic acid/C12-ester C ₁₂ H ₁₈ O ₂	Weak	0.029 (0.003-0.766)	Oxidation of biomass burning	Haeri, 2023
109	217.195	C6-substituted dihydronaphthalene C ₁₆ H ₂₄	Weak	0.026 (0.003-0.307)	asphalt degassing	Khare et al., 2020
110	233.228	C11-substituted benzene C ₁₇ H ₂₈	Weak	0.023 (0.002-0.215)	asphalt degassing	Khare et al., 2020, Xu et al. 2022
111	247.243	C12-substituted benzene C ₁₈ H ₃₀	Weak	0.022 (0.002-0.158)	asphalt degassing	Khare et al., 2020

Table S2: List of Constraints incorporated in the PMF model

Sr. No.	Factor	Element	Type
1	Biogenic	m/z 42.030	Pull Down Maximally
2	Biogenic	m/z 93.069	Pull Down Maximally
3	Biogenic	m/z 107.085	Pull Down Maximally
4	Biogenic	m/z 121.101	Pull Down Maximally
5	Biogenic	10/16/2022 11:00:00 PM	Pull Down Maximally
6	Biogenic	10/17/2022 1:00:00 AM	Pull Down Maximally
7	Biogenic	10/17/2022 12:00:00 AM	Pull Down Maximally
8	Biogenic	10/17/2022 2:00:00 AM	Pull Down Maximally
9	Biogenic	10/16/2022 10:00:00 PM	Pull Down Maximally
10	Biogenic	10/16/2022 9:00:00 PM	Pull Down Maximally

11	Biogenic	10/21/2022 10:00:00 PM	Pull Down Maximally
12	Biogenic	10/21/2022 11:00:00 PM	Pull Down Maximally
13	Biogenic	10/22/2022 12:00:00 AM	Pull Down Maximally
14	Biogenic	10/21/2022 9:00:00 PM	Pull Down Maximally
15	Biogenic	10/21/2022 8:00:00 PM	Pull Down Maximally
16	Biogenic	10/22/2022 6:00:00 PM	Pull Down Maximally
17	Biogenic	10/23/2022 7:00:00 PM	Pull Down Maximally
18	Biogenic	10/26/2022 11:00:00 PM	Pull Down Maximally
19	Photochemical	m/z 42.030	Pull Down Maximally
20	Photochemical	m/z 93.069	Pull Down Maximally
21	Photochemical	m/z 107.085	Pull Down Maximally
22	Photochemical	m/z 121.101	Pull Down Maximally
23	Photochemical	9/20/2022 2:00:00 AM	Pull Down Maximally
24	Photochemical	9/20/2022 11:00:00 PM	Pull Down Maximally
25	Photochemical	9/22/2022 1:00:00 AM	Pull Down Maximally
26	Photochemical	9/23/2022 10:00:00 PM	Pull Down Maximally
27	Photochemical	9/24/2022 1:00:00 AM	Pull Down Maximally
28	Photochemical	10/4/2022 2:00:00 AM	Pull Down Maximally
29	Photochemical	10/4/2022 4:00:00 AM	Pull Down Maximally
30	Cooking	10/17/2022 8:00:00 PM	Pull Up Maximally
31	Solvents	11/8/2022 4:00:00 AM	Pull Up Maximally
32	Road Construction	10/17/2022 9:00:00 PM	Pull Up Maximally
33	Petrol 4-Wheeler	10/18/2022 11:00:00 PM	Pull Up Maximally
34	Paddy	11/12/2022 1:00:00 AM	Pull Up Maximally
35	Paddy	11/12/2022 12:00:00 AM	Pull Up Maximally
36	Heating & Waste Disposal	11/19/2022 11:00:00 PM	Pull Up Maximally
37	Petrol 2-Wheeler	10/17/2022 9:00:00 PM	Pull Up Maximally
38	Industrial	10/16/2022 11:00:00 PM	Pull Up Maximally
39	CNG	10/16/2022 7:00:00 PM	Pull Up Maximally

Table S3: Contains the SOA yields for 53 compounds to calculate the SOAP

Sr. No.	m/z	SOAP	References
1	31.014	0.7	Derwent et. al. 2010
2	33.030	0.3	Derwent et. al. 2010
3	53.035	0.1	Derwent et. al. 2010
4	55.051	0.6	Derwent et. al. 2010
5	61.025	30.6	Xiong et. al. 2020
6	67.051	11.5	Hakkim et al. 2021
7	71.047	0.3	Derwent et. al. 2010
8	73.026	0.1	Derwent et. al. 2010
9	79.052	29.4	Hakkim et al. 2021
10	83.047	42.3	Hakkim et al. 2021, Xiong et. al. 2020
11	83.084	82.2	Hakkim et al. 2021
12	87.043	0.6	Derwent et. al. 2010
13	95.084	145.6	Chan et. al. 2009, Kılıç et. al. 2018, Hakkim et al. 2021, Xiong et. al. 2020
14	99.043	41.2	Hakkim et al. 2021
15	121.101	1	Xiong et. al. 2020
16	137.133	0.1	Derwent et. al. 2010
17	44.018	100	Chan et. al. 2009, Kılıç et. al. 2018, Hakkim et al. 2021, Xiong et. al. 2020
18	47.046	278.4	Kılıç et. al. 2018, Hakkim et al. 2021, Khare et. al. 2020
19	49.007	188.2	Hakkim et al. 2021

20	62.997	188.2	Kılıç et. al. 2018
21	85.099	83.5	Kılıç et. al. 2018, Hakkim et al. 2021, Xiong et. al. 2020
22	87.079	188.2	Kılıç et. al. 2018
23	91.053	69.4	Chan et. al. 2009, Kılıç et. al. 2018, Hakkim et al. 2021, Xiong et. al. 2020
24	97.100	229.4	Kılıç et. al. 2018
25	111.080	188.2	Kılıç et. al. 2018
26	115.039	75.3	Chan et. al. 2009, Kılıç et. al. 2018, Hakkim et al. 2021, Xiong et. al. 2020
27	119.085	117.6	Kılıç et. al. 2018
28	123.044	200	Yee et. al. 2013
29	125.060	185	Chan et. al. 2009, Kılıç et. al. 2018, Hakkim et al. 2021, Khare et. al. 2020
30	127.075	129.4	Kılıç et. al. 2018, Khare et. al. 2020
31	133.065	86.3	Kılıç et. al. 2018, Hakkim et al. 2021, Khare et. al. 2020
32	133.102	176.5	Xiong et. al. 2020
33	138.056	221.6	Chan et. al. 2009, Kılıç et. al. 2018, Khare et. al. 2020
34	145.051	88.2	Khare et. al. 2020
35	145.123	9.4	Xiong et. al. 2020
36	147.118	102.9	Kılıç et. al. 2018, Khare et. al. 2020

37	149.096	70.6	Khare et. al. 2020
38	153.128	2.5	Khare et. al. 2020
39	155.144	0.9	Khare et. al. 2020
40	157.099	176.5	Chan et. al. 2009, Khare et. al. 2020
41	161.134	114.7	Kılıç et. al. 2018, Khare et. al. 2020
42	175.150	147.1	Khare et. al. 2020
43	177.056	170.6	Khare et. al. 2020
44	177.165	147.1	Khare et. al. 2020
45	179.181	4.6	Khare et. al. 2020
46	183.121	288.2	Khare et. al. 2020
47	185.121	35.3	Witkowski et. al. 2017
48	187.148	194.1	Khare et. al. 2020
49	189.165	194.1	Khare et. al. 2020
50	191.181	194.1	Khare et. al. 2020
51	217.195	252.9	Khare et. al. 2020
52	233.228	276.5	Khare et. al. 2020
53	247.243	305.9	Khare et. al. 2020

Table S4: Correlation table (R) for the 11 factors with independent tracer species.

Tracer Species	Cooking	Solvents	Road Construction	Biogenic	Petrol 4-Wheeler	Paddy	Heating & Waste Burning	Petrol 2-Wheeler	Industrial	Photo-chemical	CNG
WS	-0.4	-0.2	-0.1	0.1	-0.3	-0.2	-0.2	-0.2	-0.3	0.0	-0.2
WD	0.1	-0.1	0.2	0.1	0.0	0.1	0.2	0.1	-0.1	0.1	0.1
CO ₂	0.2	0.2	0.1	-0.3	0.7	0.4	0.4	0.7	0.8	-0.1	0.3
N ₂ O	0.0	0.0	-0.1	-0.1	0.2	0.0	0.1	0.2	0.4	-0.1	0.2
CH ₄	0.2	0.3	0.0	-0.3	0.6	0.4	0.3	0.6	0.8	-0.1	0.3
PM ₁₀	0.3	0.2	0.1	-0.2	0.4	0.7	0.7	0.5	0.5	0.0	0.3
PM _{2.5}	0.3	0.2	0.1	-0.3	0.3	0.7	0.6	0.4	0.5	0.0	0.2
CO	0.3	0.3	0.1	-0.2	0.7	0.5	0.5	0.6	0.7	-0.1	0.4
NO	0.1	0.2	0.0	-0.2	0.8	0.3	0.4	0.5	0.7	-0.1	0.3
NO ₂	0.1	0.1	0.1	-0.2	0.3	0.3	0.7	0.4	0.2	0.0	0.2
NO _x	0.1	0.2	0.0	-0.2	0.8	0.3	0.5	0.6	0.7	-0.1	0.3
O ₃	0.1	-0.1	0.3	0.5	-0.2	0.0	-0.1	-0.2	-0.3	0.4	-0.2
SO ₂	0.0	-0.1	-0.2	-0.1	0.2	0.3	0.4	0.2	0.2	0.0	0.2
AT	0.2	-0.1	0.2	0.7	-0.2	-0.3	-0.6	-0.3	-0.4	0.3	0.1
RH	-0.1	0.1	-0.2	-0.5	0.0	-0.2	-0.4	-0.1	0.2	-0.4	-0.1
PAR	0.2	-0.2	0.2	0.7	-0.2	-0.1	-0.2	-0.3	-0.3	0.3	-0.2
VC	-0.2	-0.2	0.1	0.6	-0.3	-0.2	-0.3	-0.3	-0.4	0.2	-0.2
FC	0.4	0.3	0.2	-0.3	0.3	0.8	0.6	0.5	0.4	0.3	0.3

AT: Ambient Temperature, RH: Relative Humidity, PAR: Photosynthetic active radiation, VC: Ventilation Coefficient,

FC: Daily Fire Count

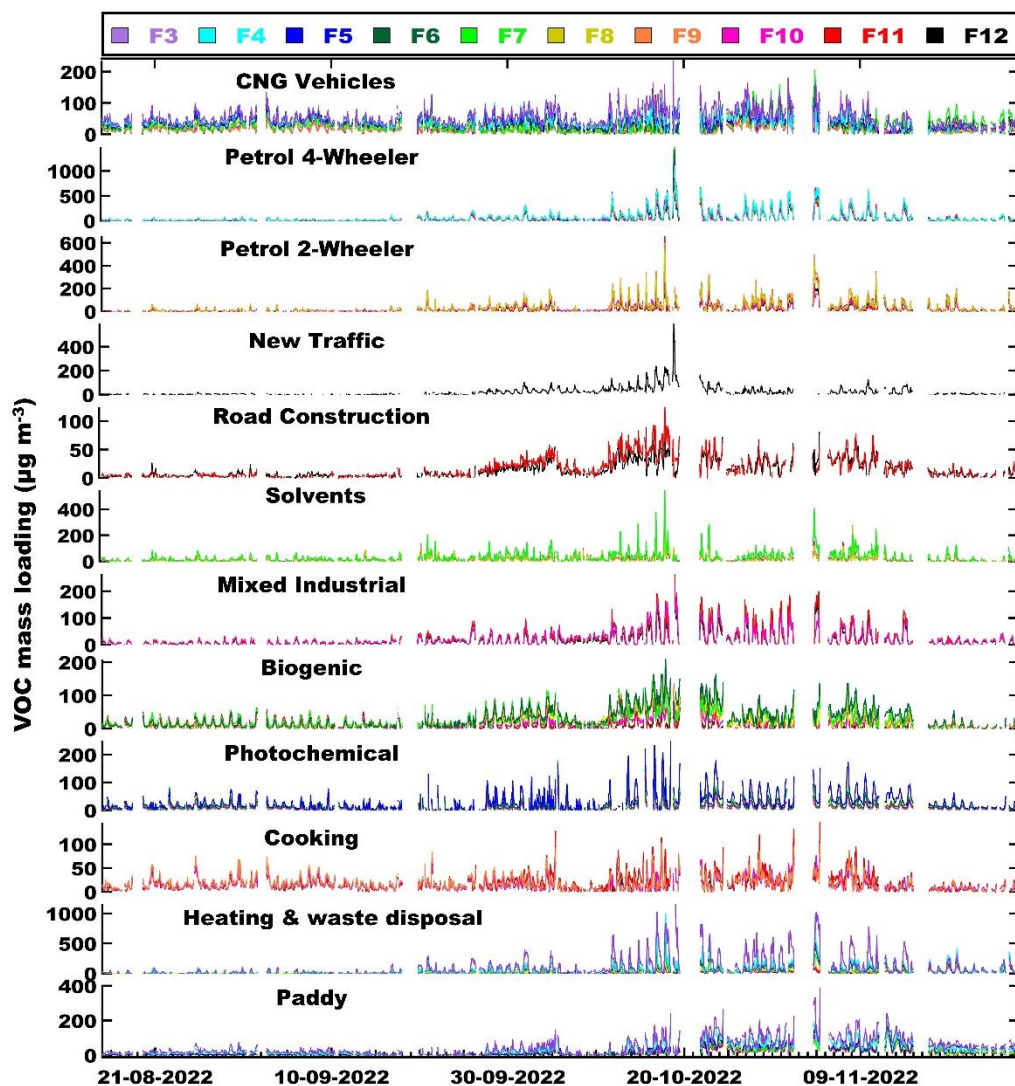


Figure S1(a): Evolution of the factor contribution time series when the number of factors is increased from 3 to 12

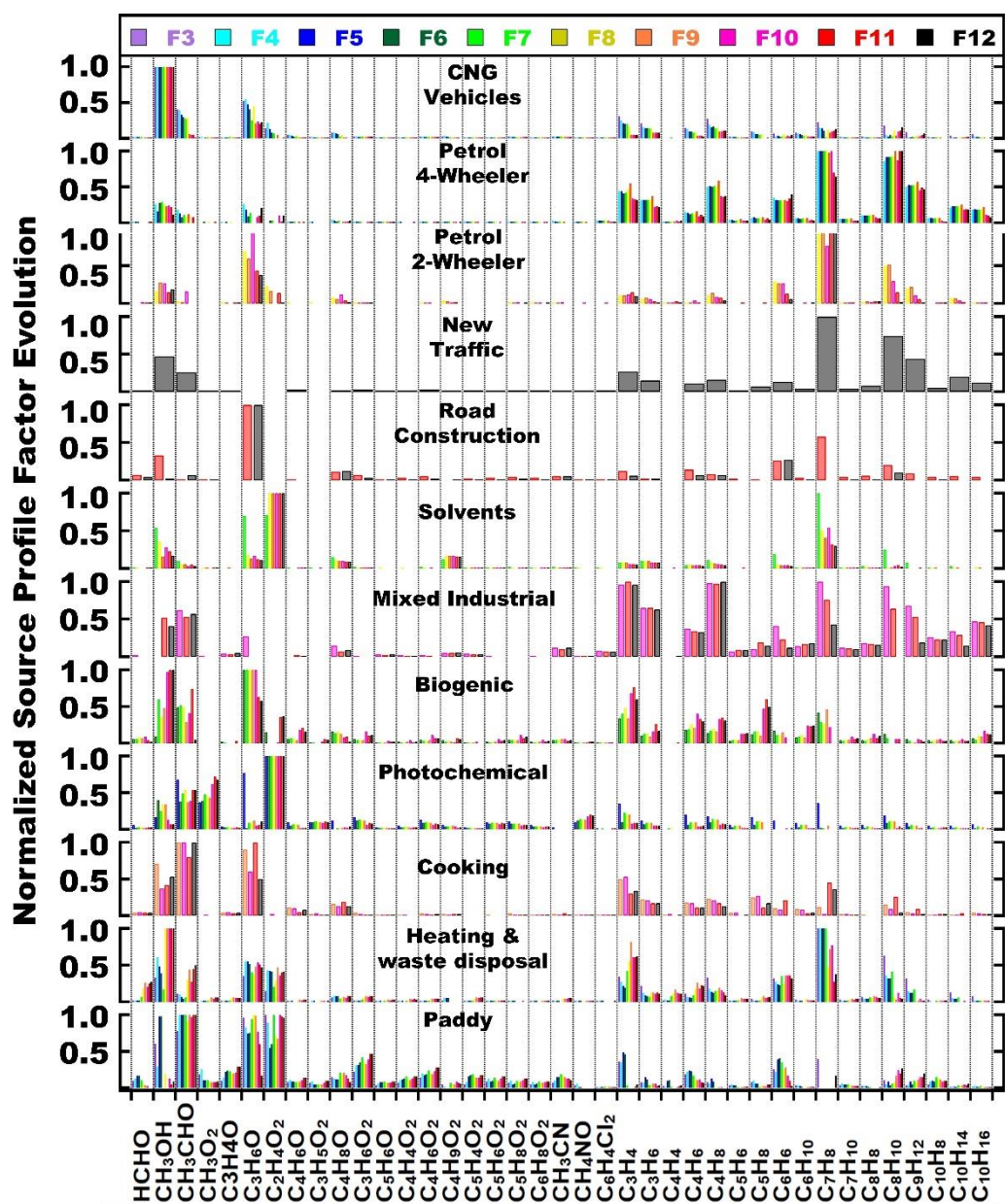


Figure S1(b): Evolution of the normalized PMF factor profile when the number of factors is increased from 3 to 12

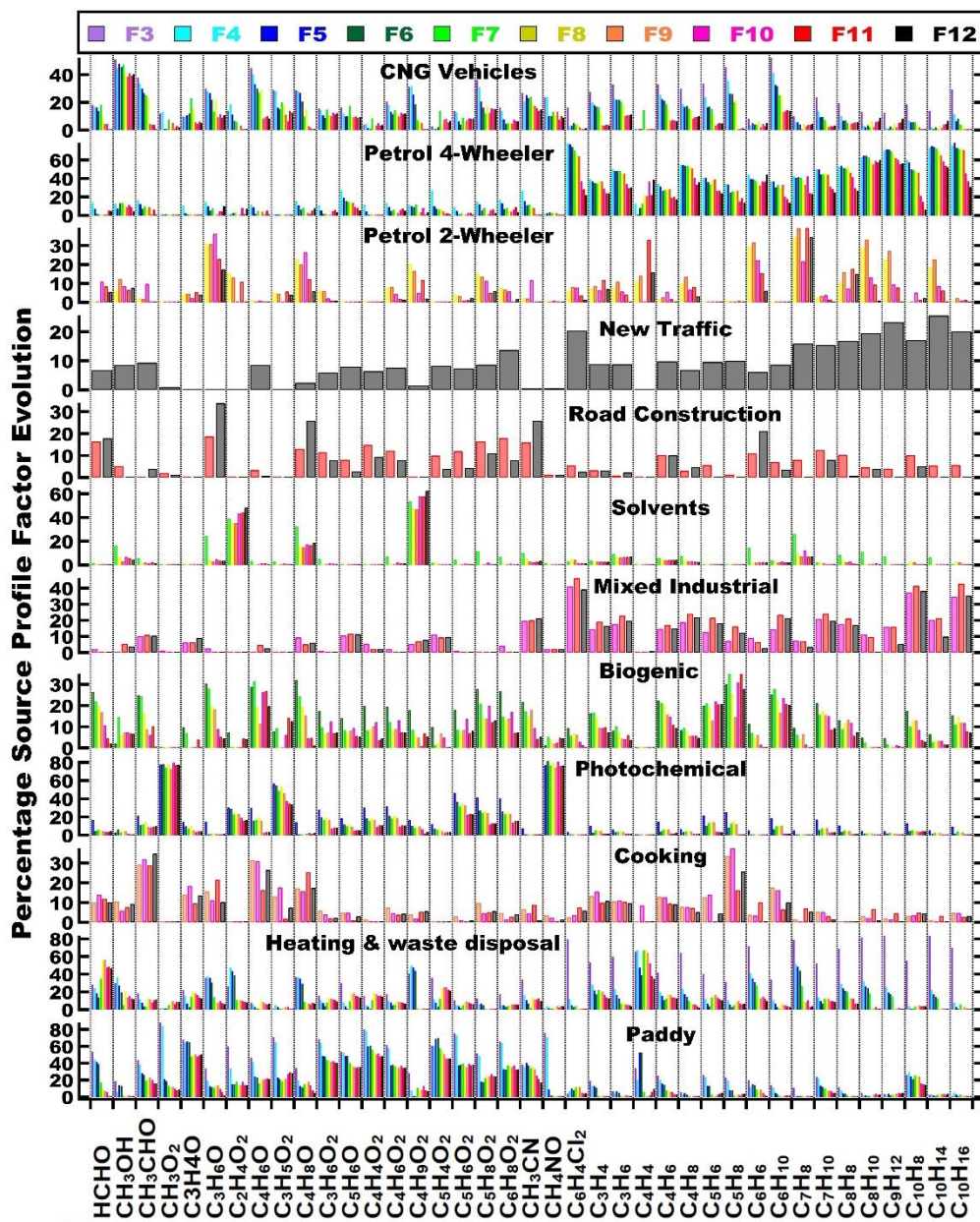


Figure S1(c): Evolution of the percentage of the mass explained by different sources when the number of factors is increased from 3 to 12

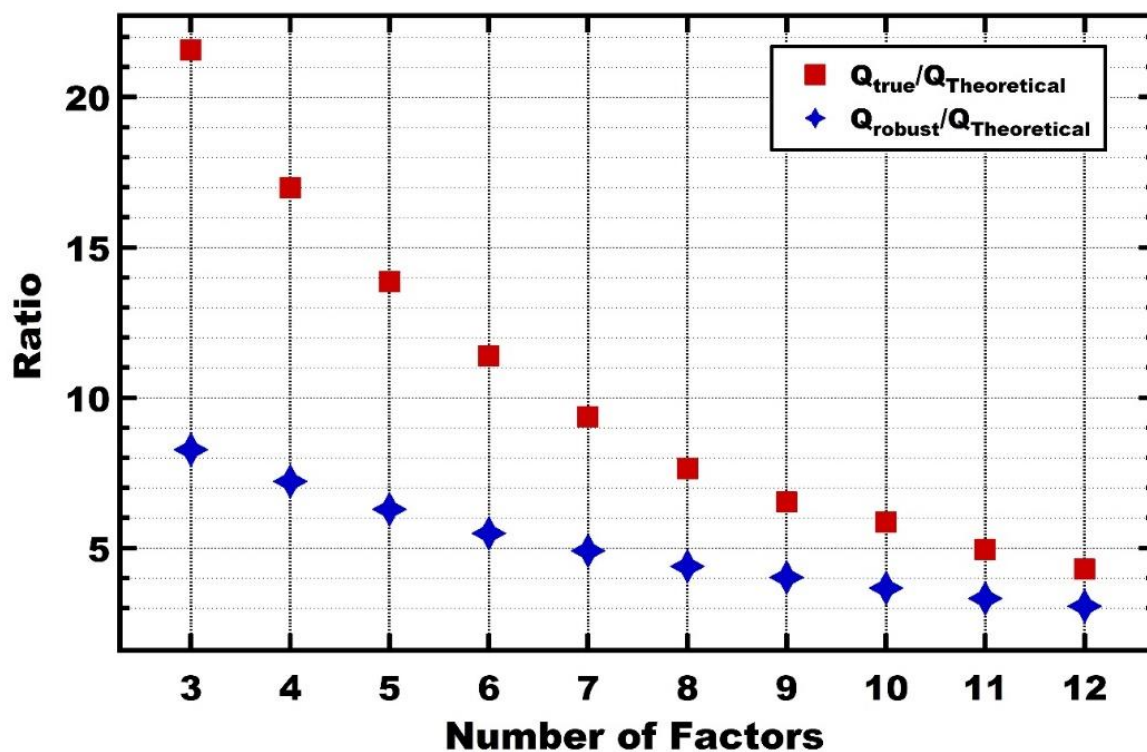


Figure S2: Change in the $Q_{\text{true}}/Q_{\text{theoretical}}$ ratio and $Q_{\text{robust}}/Q_{\text{theoretical}}$ when the number of factors is increased from 3 to 12

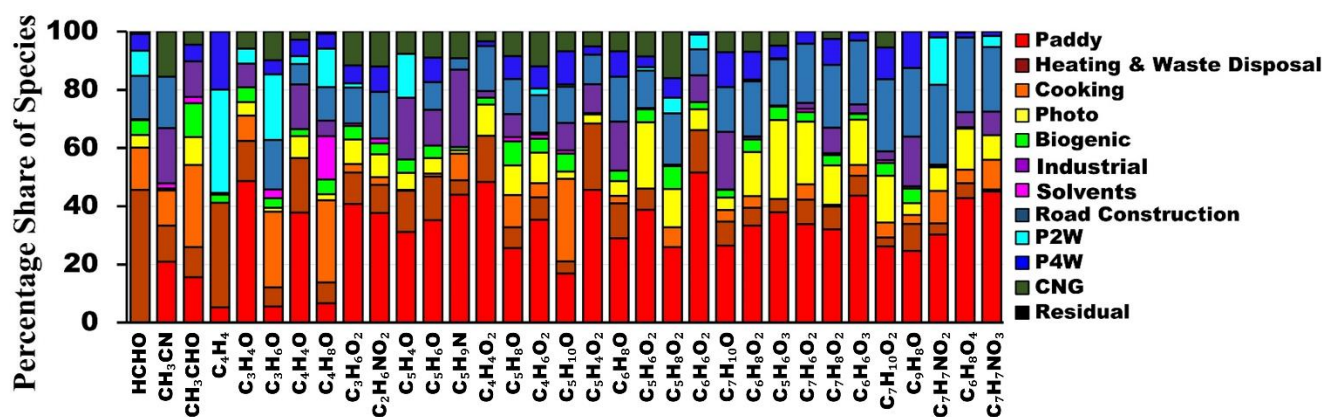


Figure S3(a): represents the share of species with the highest percentages in paddy residue burning, residential heating and waste disposal and solid fuel-based cooking factors

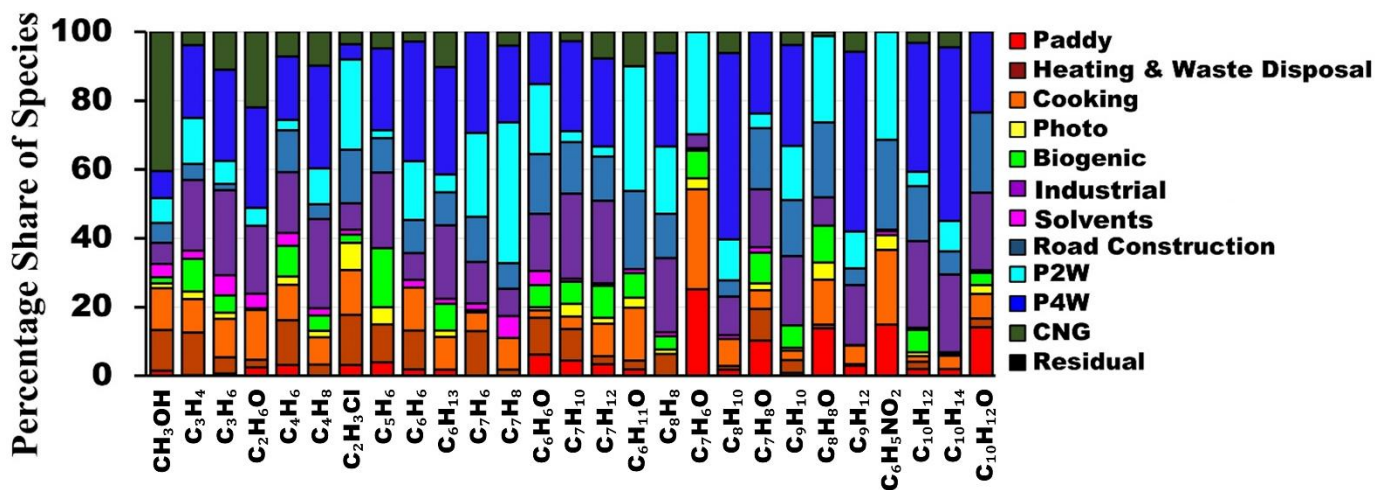


Figure S3(b): represents the share of species with the highest percentages in CNG, petrol 2-wheeler, petrol 4-wheeler factors.

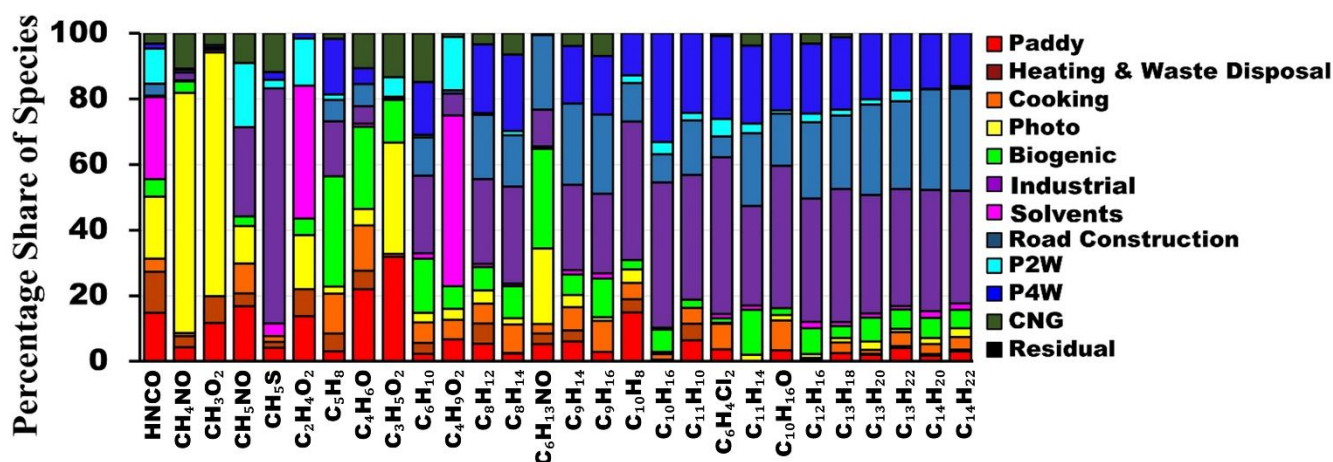


Figure S3(c): represents the share of species with the highest percentages in biogenic, photochemistry, solvents, and industrial factors.

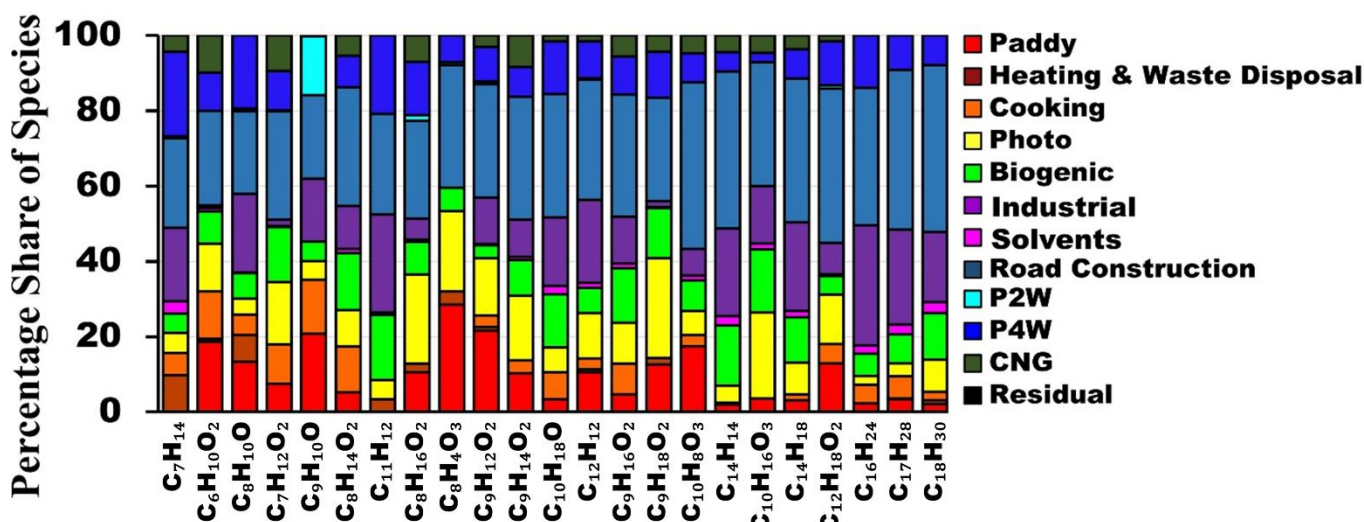


Figure S3(d): represents the share of species with the highest percentages in road construction factors.

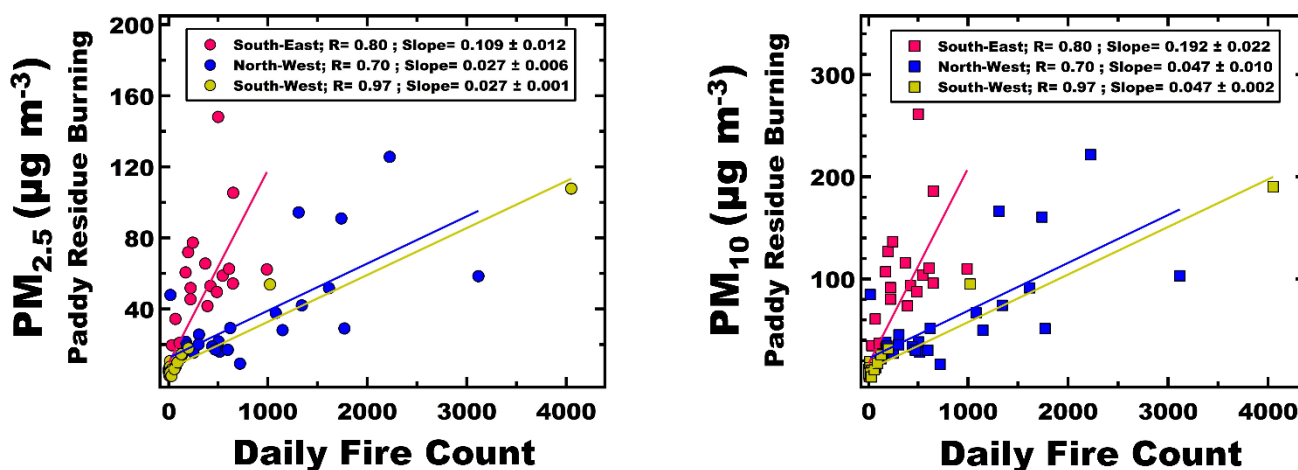


Figure S4: represents the PM_{2.5} and PM₁₀ mass loadings from the paddy residue burning factor at the receptor site influenced by the 24-hour averaged fire count in three fetch regions (SE, NW, SW).

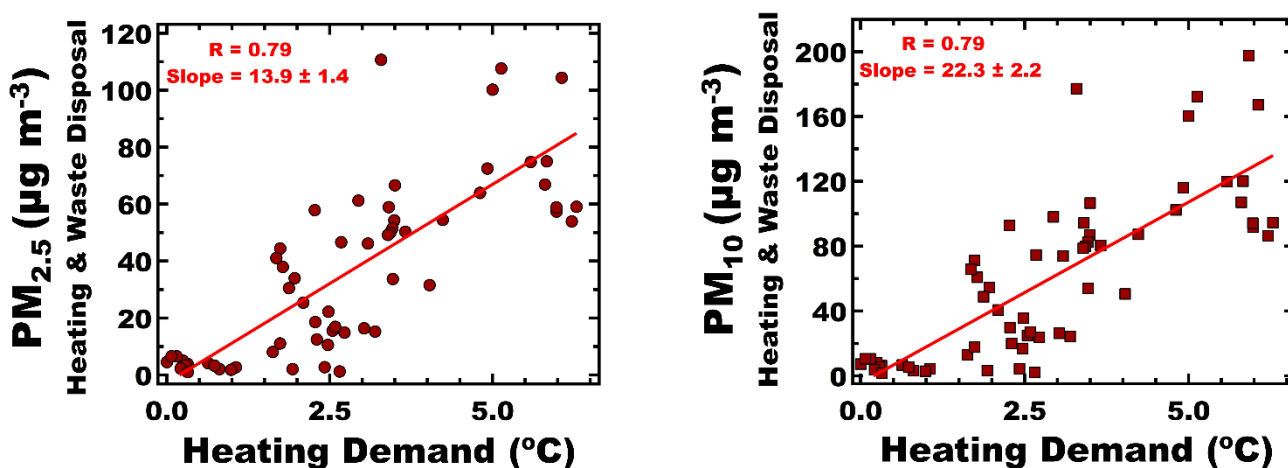


Figure S5: represents the PM_{2.5} and PM₁₀ mass loadings at the receptor site with 24-hour averaged heating demand

References:

- Bruns, E. A., Slowik, J. G., El Haddad, I., Kilic, D., Klein, F., Dommen, J., Temime-Roussel, B., Marchand, N., Baltensperger, U., and Prévôt, A. S. H.: Characterization of gas-phase organics using proton transfer reaction time-of-flight mass spectrometry: Fresh and aged residential wood combustion emissions. *Atmos. Chem. Phys.*, 17(1), 705–720, <https://doi.org/10.5194/acp-17-705-2017>, 2017.
- Camredon, M., Hamilton, J. F., Alam, M. S., Wyche, K. P., Carr, T., White, I. R., Monks, P. S., Rickard, A. R., and Bloss, W. J.: Distribution of gaseous and particulate organic composition during dark α -pinene ozonolysis, *Atmos. Chem. Phys.*, 10, 2893–2917, <https://doi.org/10.5194/acp-10-2893-2010>, 2010.
- Chan, A. W. H., Kautzman, K. E., Chhabra, P. S., Surratt, J. D., Chan, M. N., Crouse, J. D., Kürten, A., Wennberg, P. O., Flagan, R. C., and Seinfeld, J. H.: Secondary organic aerosol formation from photooxidation of naphthalene and

alkyl-naphthalenes: implications for oxidation of intermediate volatility organic compounds (IVOCs), *Atmos. Chem. Phys.*, 9, 3049–3060, <https://doi.org/10.5194/acp-9-3049-2009>, 2009.

Chandra, B. P., and Sinha, V.: Contribution of post-harvest agricultural paddy residue fires in the N.W. Indo-Gangetic Plain to ambient carcinogenic benzenoids, toxic isocyanic acid and carbon monoxide. *Environ. Int.*, 88, 187–197, <https://doi.org/10.1016/J.ENVINT.2015.12.025>, 2016.

Coggon, M. M., Lim, C. Y., Koss, A. R., Sekimoto, K., Yuan, B., Gilman, J. B., Hagan, D. H., Selimovic, V., Zarzana, K. J., Brown, S. S., Roberts, J. M., Müller, M., Yokelson, R., Wisthaler, A., Krechmer, J. E., Jimenez, J. L., Cappa, C., Kroll, J. H., De Gouw, J., and Warneke, C.: OH chemistry of non-methane organic gases (NMOGs) emitted from laboratory and ambient biomass burning smoke: evaluating the influence of furans and oxygenated aromatics on ozone and secondary NMOG formation. *Atmos. Chem. Phys.*, 19, 14875–14899, <https://doi.org/10.5194/acp-19-14875-2019>, 2019.

Derwent, R. G., Jenkin, M. E., Saunders, S. M., and Pilling, M. J.: Photochemical ozone creation potentials for organic compounds in northwest Europe calculated with a master chemical mechanism. *Atmos. Environ.*, 32(14–15), 2429–2441, [https://doi.org/10.1016/S1352-2310\(98\)00053-3](https://doi.org/10.1016/S1352-2310(98)00053-3), 1998.

Derwent, R. G., Jenkin, M. E., Utembe, S. R., Shallcross, D. E., Murrells, T. P., and Passant, N. R.: Secondary organic aerosol formation from a large number of reactive man-made organic compounds. *Sci. Total. Environ.*, 408(16), 3374–3381, <https://doi.org/10.1016/J.SCITOTENV.2010.04.013>, 2010.

Fleming, L. T., Weltman, R., Yadav, A., Edwards, R. D., Arora, N. K., Pillarisetti, A., Meinardi, S., Smith, K. R., Blake, D. R., and Nizkorodov, S. A.: Emissions from village cookstoves in Haryana, India, and their potential impacts on air quality, *Atmos. Chem. Phys.*, 18, 15169–15182, <https://doi.org/10.5194/acp-18-15169-2018>, 2018.

Fukusaki, Y., Kousa, Y., Umehara, M., Ishida, M., Sato, R., Otagiri, K., Hoshi, J., Nudjima, C., Takahashi, K., and Nakai, S.: Source region identification and source apportionment of volatile organic compounds in the Tokyo Bay coastal area, *Japan. Atmos. Environ.: X*, 9, <https://doi.org/10.1016/j.aeaoa.2021.100103>, 2021.

Gkatzelis, G. I., Hohaus, T., Tillmann, R., Gensch, I., Müller, M., Eichler, P., Xu, K.-M., Schlag, P., Schmitt, S. H., Yu, Z., Wegener, R., Kaminski, M., Holzinger, R., Wisthaler, A., and Kiendler-Scharr, A.: Gas-to-particle partitioning of major biogenic oxidation products: a study on freshly formed and aged biogenic SOA, *Atmos. Chem. Phys.*, 18, 12969–12989, <https://doi.org/10.5194/acp-18-12969-2018>, 2018.

Guenther, A., Karl, T., Harley, P., Wiedinmyer, C., Palmer, P. I., and Geron, C.: Estimates of global terrestrial isoprene emissions using MEGAN (Model of Emissions of Gases and Aerosols from Nature). *Atmos. Chem. Phys.*, 6(11), 3181–3210, <https://doi.org/10.5194/ACP-6-3181-2006>, 2006.

Haeri, F.: Molecular Speciation of Organic Nitrogen Compounds Separated in Smoke Particles Emitted from Burning Western U.S. Wildland Fuels, PhD thesis, Carnegie Mellon University, Pittsburgh, PA, USA, <https://doi.org/10.1184/R1/22670578.v1>, 2023.

Hakkim, H., Kumar, A., Annadate, S., Sinha, B., and Sinha, V.: RTEII: A new high-resolution ($0.1^\circ \times 0.1^\circ$) road transport emission inventory for India of 74 speciated NMVOCs, CO, NO_x, NH₃, CH₄, CO₂, PM_{2.5} reveals massive overestimation of NO_x and CO and missing nitromethane emissions by existing inventories. *Atmos. Environ.: X*, 11, 100118, <https://doi.org/10.1016/J.AEAOA.2021.100118>, 2021.

Harrison, M. A., Barra, S., Borghesi, D., Vione, D., Arsene, C., and Olariu, R. I.: Nitrated phenols in the atmosphere: a review. *Atmos. Environ.*, 39(2), 231–248, <https://doi.org/10.1016/j.atmosenv.2004.09.044>, 2005.

Hatch, L. E., Luo, W., Pankow, J. F., Yokelson, R. J., Stockwell, C. E., and Barsant K. C.: Identification and quantification of gaseous organic compounds emitted from biomass burning using two-dimensional gas chromatography–time-of-flight mass spectrometry. *Atmos. Chem. Phys.*, 15, 1865–1899, <https://doi.org/10.5194/acp-15-1865-2015>, 2015.

Hatch, L. E., Yokelson, R. J., Stockwell, C. E., Veres, P. R., Simpson, I. J., Blake, D. R., Orlando, J. J., and Barsanti K. C.: Multi-instrument comparison and compilation of non-methane organic gas emissions from biomass burning and implications for smoke-derived secondary organic aerosol precursors. *Atmos. Chem. Phys.*, 17, 1471–1489, <https://doi.org/10.5194/acp-17-1471-2017>, 2017.

Hsu, C. Y., Wu, P. Y., Chen, Y. C., Chen, P. C., Guo, Y. L., Lin, Y. J., and Lin, P.: An integrated strategy by using long-term monitoring data to identify volatile organic compounds of high concern near petrochemical industrial parks. *Sci. Total Environ.*, 821, <https://doi.org/10.1016/j.scitotenv.2022.153345>, 2022.

Jordan, C., Fitz, E., Hagan, T., Sive, B., Frinak, E., Haase, K., Cottrell, L., Buckley, S., and Talbot, R.: Long-term study of VOCs measured with PTR-MS at a rural site in New Hampshire with urban influences. *Atmos. Chem. Phys.*, 9(14), 4677–4697, <https://doi.org/10.5194/ACP-9-4677-2009>, 2009.

Kamarulzaman, N. H., Le-Minh, N., and Stuetz, R. M.: Identification of VOCs from natural rubber by different headspace techniques coupled using GC-MS. *Talanta*, 191, 535–544, <https://doi.org/10.1016/j.talanta.2018.09.019>, 2019.

Khare, P., Machesky, J., Soto, R. He, M., Presto, A. A. and Gentner, D. R.: Asphalt-related emissions are a major missing nontraditional source of secondary organic aerosol precursors. *Science Advances* 6, eabb9785, <https://doi.org/10.1126/sciadv.abb9785>, 2020.

Kılıç, D., El Haddad, I., Brem, B. T., Bruns, E., Bozetti, C., Corbin, J., Durdina, L., Huang, R.-J., Jiang, J., Klein, F., Lavi, A., Pieber, S. M., Rindlisbacher, T., Rudich, Y., Slowik, J. G., Wang, J., Baltensperger, U., and Prévôt, A. S. H.: Identification of secondary aerosol precursors emitted by an aircraft turbofan, *Atmos. Chem. Phys.*, 18, 7379–7391, <https://doi.org/10.5194/acp-18-7379-2018>, 2018.

Koss, A. R., Sekimoto, K., Gilman, J. B., Selimovic, V., Coggon, M. M., Zarzana, K. J., Yuan, B., Lerner, B. M., Brown, S. S., Jimenez, J. L., Krechmer, J., Roberts, J. M., Warneke, C., Yokelson, R. J., and De Gouw, J.: Non-methane organic gas emissions from biomass burning: Identification, quantification, and emission factors from PTR-ToF during the FIREX 2016 laboratory experiment. *Atmos. Chem. Phys.*, 18(5), 3299–3319, <https://doi.org/10.5194/ACP-18-3299-2018>, 2018.

Kumar, A., Hakkim, H., Sinha, B., and Sinha, V.: Gridded 1 km × 1 km emission inventory for paddy stubble burning emissions over north-west India constrained by measured emission factors of 77 VOCs and district-wise crop yield data. *Sci. Total Environ.*, 789, 148064, <https://doi.org/10.1016/J.SCITOTENV.2021.148064>, 2021.

Kumar, A., Sinha, V., Shabin, M., Hakkim, H., Bonsang, B., and Gros, V.: Non-methane hydrocarbon (NMHC) fingerprints of major urban and agricultural emission sources for use in source apportionment studies. *Atmos. Chem. Phys.*, 20(20), 12133–12152, <https://doi.org/10.5194/ACP-20-12133-2020>, 2020.

Lignell, H., Epstein, S. A., Marvin, M. R., Shemesh, D., Gerber, B., and Nizkorodov, S.: Experimental and Theoretical Study of Aqueous cis-Pinonic Acid Photolysis. *J. Phys. Chem. A* 2013, 117, 12930–12945, <https://doi.org/10.1021/jp4093018>, 2013.

Loubet, B., Buysse, P., Gonzaga-Gomez, L., Lafouge, F., Ciuraru, R., Decuq, C., Kammer, J., Bsaibes, S., Boissard, C., Durand, B., Gueudet, J.-C., Fanucci, O., Zurfluh, O., Abis, L., Zannoni, N., Truong, F., Baisnée, D., Sarda-Estève, R., Staudt, M., and Gros, V.: Volatile organic compound fluxes over a winter wheat field by PTR-Qi-TOF-MS and eddy covariance, *Atmos. Chem. Phys.* 22, 2817–2842, <https://doi.org/10.5194/acp-22-2817-2022>, 2022.

Mochizuki, T., Kawamura, K., Miyazaki, Y., Kunwar, B., and Boreddy, S. K. R.: Distributions and sources of low-molecular-weight monocarboxylic acids in gas and particles from a deciduous broadleaf forest in northern Japan. *Atmos. Chem. Phys.*, 19(4), 2421–2432, <https://doi.org/10.5194/acp-19-2421-2019>, 2019.

Nowakowska, M., Herbinet, O., Dufour, A., and Glaude, P. A.: Kinetic Study of the Pyrolysis and Oxidation of Guaiacol. *J. Phys. Chem. A*, 122(39), 7894–7909, <https://doi.org/10.1021/acs.jpca.8b06301>, 2018.

Palm, B., Peng, Q., Fredrickson, C. D., Lee B. H., Garofalo, L. A., Pothier, M. A., Kreidenweis S. M., Farmer D. K., Pokhrel, R. P., Shen, Y., Murphy S. M., Permar W., Hu L. Campos T.L., Hall S. R., Ullmann K., Zhang, X., Flocke, F., Fischer, E. V., and Thornton, J. A.: Quantification of organic aerosol and brown carbon evolution in fresh wildfire plumes. *P. Natl. Acad. Sci. USA*, 117 (47) 29469–29477, <https://doi.org/10.1073/pnas.2012218117>, 2020.

Ramasamy, S., Nakayama, T., Imamura, T., Morino, Y., Kajii, Y. and Sato, K.: Investigation of dark condition nitrate radical- and ozone-initiated aging of toluene secondary organic aerosol: Importance of nitrate radical reactions with phenolic products. *Atmos. Environ.* 219, 117049, <https://doi.org/10.1016/j.atmosenv.2019.117049>, 2019.

Sarkar, C., Sinha, V., Kumar, V., Rupakheti, M., Panday, A., Mahata, K. S., Rupakheti, D., Kathayat, B., and Lawrence, M. G.: Overview of VOC emissions and chemistry from PTR-TOFMS measurements during the SusKat-ABC campaign: high

acetaldehyde, isoprene and isocyanic acid in wintertime air of the Kathmandu Valley. *Atmos. Chem. Phys.*, 16, 3979–4003, <https://doi.org/10.5194/acp-16-3979-2016>, 2016.

Sarkar, C., Sinha, V., Sinha, B., Panday, A. K., Rupakheti, M., and Lawrence, M. G.: Source apportionment of NMVOCs in the Kathmandu Valley during the SusKat-ABC international field campaign using positive matrix factorization. *Atmos. Chem. Phys.*, 17(13), 8129–8156, <https://doi.org/10.5194/ACP-17-8129-2017>, 2017.

Stockwell, C. E., Veres, P. R., Williams, J., and Yokelson, R. J.: Characterization of biomass burning emissions from cooking fires, peat, crop residue, and other fuels with high-resolution proton-transfer-reaction time-of-flight mass spectrometry. *Atmos. Chem. Phys.*, 15, 845–865, <https://doi.org/10.5194/acp-15-845-2015>, 2015.

Toda, K., Obata, T., Obokin, V. A., Potemkin, V. L., Hirota, K., Takeuchi, M., Arita, S., Khodzher, T. V., and Grachev, M. A.: Atmospheric methanethiol emitted from a pulp and paper plant on the shore of Lake Baikal, *Atmos. Environ.*, 44, 2427–2433, <https://doi.org/10.1016/j.atmosenv.2010.03.037>, 2010.

Wang, Z., Yuan, B., Ye, C., Roberts, J., Wisthaler, A., Lin, Y., Li, T., Wu, C., Peng, Y., Wang, C., Wang, S., Yang, S., Wang, B., Qi, J., Wang, C., Song, W., Hu, W., Wang, X., Xu, W., ... Shao, M.: High Concentrations of Atmospheric Isocyanic Acid (HNCO) Produced from Secondary Sources in China. *Environ. Sci. Technol.*, 54(19), 11818–11826, <https://doi.org/10.1021/acs.est.0c02843>, 2020.

Wang, M., Wang, Q., Ho, S. S. H., Li, H., Zhang, R., Ran, W., Que, L.: Chemical characteristics and sources of nitrogen-containing organic compounds at a regional site in the North China Plain during the transition period of autumn and winter. *Sci. Total. Environ.*, 812, 151451, <https://doi.org/10.1016/j.scitotenv.2021.151451>, 2022.

Witkowski, B., and Gierczak, T.: cis-Pinonic acid oxidation by hydroxyl radicals in the aqueous phase under acidic and basic conditions: kinetics and mechanism. *Environ. Sci. Technol.*, 51(17), 9765–9773, <https://doi.org/10.1021/acs.est.7b02427>, 2017.

Xing, C., Wan, Y., Wang, Q., Kong, S., Huang, X., Ge, X., et al.: Molecular characterization of brown carbon chromophores in atmospherically relevant samples and their gas-particle distribution and diurnal variation in the atmosphere. *J. Geophys. Res.-Atmos.*, 128, e2022JD038142, <https://doi.org/10.1029/2022JD038142>, 2023.

Xiong, Y., Zhou, J., Xing, Z., and Du, K.: Optimization of a volatile organic compound control strategy in an oil industry center in Canada by evaluating ozone and secondary organic aerosol formation potential. *Environ. Res.*, 191, 110217, <https://doi.org/10.1016/j.envres.2020.110217>, 2020.

Xu, C., Gao, L., Lyu, C., Qiao, L., Huang, D., Liu, Y., Li, D. and Zheng, M.: Molecular characteristics, sources and environmental risk of aromatic compounds in particulate matter during COVID-2019: Nontarget screening by ultra-high resolution mass spectrometry and comprehensive two-dimensional gas chromatography. *Environ. Int.*, 167, 107421, <https://doi.org/10.1016/j.envint.2022.107421>, 2022.

Yáñez-Serrano, A. M., Filella, I., LLusià, J., Gargallo-Garriga, A., Granda, V., Bourtsoukidis, E., Williams, J., Seco, R., Cappellin, L., Werner, C., de Gouw, J., and Peñuelas, J.: GLOVOCS - Master compound assignment guide for proton transfer reaction mass spectrometry users. *Atmos. Environ.*, 244, 117929, <https://doi.org/10.1016/J.ATMOSENV.2020.117929>, 2021.

Yao, L., Wang, M.-Y., Wang, X. -K., Liu, Y.-J., Chen, H.-F., Zheng, J., Nie, W., Ding, A.-J., Geng, F.-H., Wang, D.-F., Chen, J.-M., Worsnop, D. R. and Wang, L.: Detection of atmospheric gaseous amines and amides by a high-resolution time-of-flight chemical ionization mass spectrometer with protonated ethanol reagent ions. *Atmos. Chem. Phys.*, 16, 14527–14543. <https://doi.org/10.5194/acp-16-14527-2016>, 2016.

Zaytsev, A., Koss, A. R., Breitenlechner, M., Krechmer, J. M., Nihill, K. J., Lim, C. Y., Rowe, J. C., Cox, J. L., Moss, J., Roscioli, J. R., Canagaratna, M. R., Worsnop, D. R., Kroll, J. H., and Keutsch, F. N.: Mechanistic Study of Formation of Ring-retaining and Ring-opening Products from Oxidation of Aromatic Compounds under Urban Atmospheric Conditions. *Atmos. Chem. Phys.*, 19, 15117–15129, <https://doi.org/10.5194/acp-19-15117-2019>, 2019.